NASA CONTRACTOR REPORT

NASA CR-2265

NASA CR-2265

EXPERIMENTAL INVESTIGATION OF ORTHOTROPIC PANEL FLUTTER AT ARBITRARY YAW ANGLES, AND COMPARISON WITH THEORY

by Peter Shyprykevich

Prepared by
GRUMMAN AEROSPACE CORPORATION
Bethpage, N.Y. 11714
for Langley Research Center

NATIONAL AERONAUTICS AND SPACE ADMINISTRATION • WASHINGTON, D. C. • MAY 1973

EXPERIMENTAL INVESTIGATION OF ORTHOTROPIC PANEL FLUTTER AT ARBITRARY YAW ANGLES, AND COMPARISON WITH THEORY

By Peter Shyprykevich
Grumman Aerospace Corporation

SUMMARY

Flutter characteristics for yaw angles between 15° and 90° were determined experimentally for two types of corrugation-stiffened panels: those with weak twisting stiffness and those with strong twisting stiffness. By mounting the panels on a remotely controlled turntable, good definition of the flutter boundaries was obtained by rotating the panels into and out of flutter. Flutter tests were conducted at M = 2 and M = 1.6 in the Langley Unitary Plan Wind Tunnel. Before flutter testing, vibration tests and analyses were also performed. The experimental flutter data is compared with flutter theory for orthotropic panels utilizing quasi-steady aerodynamics. In total, five different corrugated panels were tested consisting of one single skin panel having a length-to-width ratio of 5 on clamped supports and four different square double skin panels on discrete flexible supports. The investigation indicated that flutter speed for corrugated panels is highly dependent on yaw angle. Reasonable flutter correlation between analysis and test was obtained for moderate yaw angles but extreme sensitivity to structural parameters made the correlation at large yaw angles uncertain.

INTRODUCTION

A candidate for the thermal protection system of high speed reentry and hypersonic vehicles is the corrugated metallic panel constructed of high temperature alloy. Such a panel may be idealized as an orthotropic plate with either flexible or rigid supports. Flexible supports are often necessary to accommodate thermal expansion without creating large thermal stresses. Ideally, such a panel would be aligned on the vehicle with the corrugations parallel to the air flow. However in a typical flight trajectory various degrees of cross flow will be encountered which, analysis indicates, may reduce flutter margins drastically (ref. 1). Since available wind tunnel data were insufficient to substantiate these analytical predictions, a test program was conducted to provide such data. Specifically, various types of orthotropic panels were designed, analyzed, fabricated, and tested in the Unitary Plan Wind Tunnel at the NASA Langley Research Center. The results of this test program and the comparison with theory are the basis of this report.

Many individuals at Grumman contributed to the work reported herein. The author wishes to acknowledge the efforts of Mr. John Valentine in designing the panel models, Mr. Edward Leszak for supervising the manufacture of the panels, and Messrs. Edward Ham, Timothy Foley, Anthony Longano and Paul Chase for testing the panels. The author is also grateful to Mr. John Smedfjeld for advice and suggestions.

NOMENCLATURE

a	panel length (x-direction, fig. 8)
b	panel width (y-direction, fig. 8)

D_1	$\frac{D_x}{1 - \mu_x \mu_y}$
D_2	$\frac{D_y}{1 - \mu_x \mu_y}$
D_{12}	$D_{xy} + \mu_x D_2$
D_x, D_y	panel bending stiffnesses in x- and y- directions, respectively
D_{xy}	panel twisting stiffness
f	frequency
f_{cr}	flutter frequency
K_D, K_R, K_T	deflectional, rotational, and torsional spring constants, respectively, per unit length
$\bar{K}_D$	$\frac{K_D}{D_1}\left(\frac{a}{\pi}\right)^3$ non-dimensional deflectional spring constant
$\bar{K}_R$	$\frac{K_R\, a}{D_1\, \pi}$ non-dimensional rotational spring constant
$\bar{K}_T$	$\frac{K_T\, a}{D_1\, \pi}$ non-dimensional torsional spring constant
M	Mach number
m,n	number of half-waves in x,y directions, respectively
P	pressure
$P_{\mathbb{C}}$	pressure of center of turntable
q	dynamic pressure of airstream
q_{cr}	dynamic pressure of airstream at flutter
x,y	Cartesian coordianates of panel (fig. 8)
β	$\sqrt{M^2 - 1}$
Λ	yaw angle
λ	dynamic pressure parameter, $\frac{2qa^3}{\beta D_1}$

λ_{cr} dynamic pressure parameter at flutter

μ_x, μ_y Poisson's ratio associated with curvature in y- and x-directions, respectively

TEST APPARATUS

Panels

The test panels (aluminum) were designed to simulate various stiffness parameters and support conditions. The summary of panel types is given in table 1. The single skin panel is representative of the torsionally weak construction, and the double skin panel of the torsionally strong construction. The single skin panel was formed from a 0.0254 cm (0.01 in.) sheet, and was bolted directly to a 1.27 cm (0.5 in.) thick aluminum supporting plate as shown in figure 1. The bolt spacing was 2.54 cm (1.0 in.). The double skin panels were formed from 0.0203 cm (0.008 in.) sheets, and joined by spot welding along their lengths at the flat part between corrugations. Except for the different cross-sections, the double skin panels were identical in construction and were similarly supported. These panels were bolted directly to the circular supporting plate on two opposite sides and mounted on discrete flexible clips on the other two sides, as shown in figure 2. The clips were attached to the supporting plate (fig. 3) with either both the inner and outer screws or with just the outer screws. This provided two different support stiffnesses. Since the clips were manufactured in two thicknesses, 0.0595 cm (0.024 in.) and 0.0457 cm (0.018 in.), a total of four different spring stiffnesses were available. In order to evaluate the effect of beading on panel flutter the double skin panel with the flat cover sheet was tested twice, once with the flat side exposed to the flow and the second time with the corrugations exposed to the flow.

As shown previously, the test panels were mounted on a circular plate which was attached to a turntable. For the double skin panels, fairings were

provided to smooth the air flow over the panel. The single skin panel corrugations were closed out at the ends and thus this panel did not require fairings. The turntable itself was mounted in the splitter plate which was projected into the airstream from the tunnel sidewall so that the tests were conducted free of the tunnel boundary layer. The whole arrangement (with a double skin panel installed) is shown in figure 4. The cavity pressure behind the panel was controlled manually by a 2.54 cm (1.0 in.) diameter line attached to a vacuum pump.

Instrumentation and Data Acquisition

Each panel specimen was instrumented with eight single-arm strain gages and five iron-constantan thermocouples. The locations of the strain gages and thermocouples are shown in figure 5 for the single skin panel and for a typical double skin panel. In addition, two flexible supports of each thickness were instrumented with strain gages.

Signals from the strain gages were used during testing to detect the onset of panel flutter and to measure flutter frequency. They were monitored on an oscillograph and a dual beam oscilloscope. The signals from the thermocouples were recorded on a Brown multi-point recorder, and observed during test to assure that temperature differential was a minimum during measurement of the flutter threshold. All monitoring and recording was done at the side of the wind-tunnel test section containing the viewing window, so that yaw angle could be measured visually and the observation of the specimen could be maintained throughout the tests. High speed 16 mm movies were also taken to record panel motion.

In addition to panel instrumentation, a calibration plate (similar to panel supporting plates) with eleven pressure taps was installed in the turntable to measure pressure variation over the panel. Seven pressure taps were located along the centerline of the turntable in the direction of the flow. Spacing of these taps was 8.89 cm (3.5 in.). Pressures were recorded

on a scanivalve system for M = 2 and M = 1.6 and for the wind-tunnel range of dynamic pressures.

Wind Tunnel

Flutter tests were conducted in the Langley Unitary Plan Wind Tunnel at Mach numbers 2 and 1.6. The dynamic pressure in that tunnel is continuously variable. The maximum levels attained at Mach numbers 2 and 1.6 were 85.1 kN/m^2(1779 psf) and 70.6 kN/m^2(1475 psf), respectively. The wind tunnel static temperature varied between 311°K and 328°K (100 to 130°F).

TEST PROCEDURE

Vibration and Static Tests

Vibration surveys and static tests were performed to check panel and support stiffnesses. For the vibration surveys, the panels were mounted in the circular supporting plate and excited by one or two air shakers. Node lines were determined using a deflectometer mounted on a movable arm. These tests were conducted without simulating the effect of the cavity. Once the panels were in the turntable on the splitter plate, the shake tests were repeated at ambient pressure to determine the effects of the actual cavity. No appreciable change in frequencies was observed. Clip flexibilities were also checked statically by loading the clip with forces and moments and measuring the resulting displacements and rotations.

Flutter Tests

Before the test models were inserted into the airstream, the calibration plate with the pressure taps was installed in the turntable. Steady-state

pressure distributions were measured over the turntable area where panel models were to be located. These pressures were used to determine pressure loading on the panels, and the cavity pressure setting which would result in zero average differential loading. The measured pressure distributions for four different dynamic pressures levels at M = 2 and M = 1.6 are shown in figure 6. All values are relative to the pressure at the center of the turntable. Low pressure variations over the panel were obtained at M = 2 at low and intermediate dynamic pressures. However, large pressure variations existed at M = 1.6 and M = 2 at high dynamic pressure levels.

For the first three panels tested, flutter boundaries were obtained for Mach numbers 2 and 1.6. However, it was determined from the data that the effect of Mach number on flutter speed corresponded to the well known factor of $1/\beta$. Thus, tests at M = 1.6 were abandoned, since at M = 2.0 the tunnel was smoother and the cavity pressure could be better controlled. The usual test procedure consisted of establishing constant temperature, dynamic pressure, and Mach number, and then rotating the panel away from the stiffest direction until flutter was initiated. During this time, cavity pressure was manipulated to maintain zero average pressure loading on the panel. At a particular dynamic pressure, a flutter point was defined as the smallest angle at which flutter could be induced by changing cavity pressure. Once the flutter point was reached, the panel was rotated back toward the stiffest direction, and the dynamic pressure increased by a certain increment. This procedure was continued until the maximum wind-tunnel dynamic pressure was attained. In this way the flutter boundary as a function of yaw angle was obtained. Additional check points were obtained by lowering the dynamic pressure by increments and repeating the above procedure. Since the turntable was power-driven, quick excursions into and out of flutter were possible. A typical trace of a strain gage response before and after initiation of flutter is shown in figure 7.

RESULTS AND DISCUSSION

Experimental and Analytical Frequency Comparisons

The combinations of panels and support stiffnesses studied are listed in table 2, and the corresponding measured and calculated frequencies are given in table 3. The coordinate system and the various panel and support parameters are defined in figure 8. Panel stiffness properties were computed using the method of reference 2, and clip stiffness properties were calculated using strain energy methods. Natural frequencies were then obtained using a Galerkin-type solution (ref. 3).

For panel 1, measured frequencies in the long direction, m, fall between the simple-clamped and clamped-clamped calculated values. This indicates that although the panel is essentially clamped along its long sides (x-edges), its short sides (y-edges) have a finite rotational restraint. Unfortunately, at the present time, the theory is incapable of analyzing flexible-clamped plates, and the actual degree of fixity was not determined analytically. In the short direction, the poor correlation is due to the difficulty in obtaining test modes and to the additional stiffness provided by the beads.

For panels 2 through 5, except for the fundamental mode, the initial comparison of frequencies between test and analysis was poor. Since the measured individual clip deflection spring constant compared very well with the calculated value, the more doubtful values of rotational and torsional spring constants were changed to improve correlation. Clip stiffness properties corresponding to the "best fit" with the measured frequencies are listed in the last column of table 2, and the resulting frequencies in the last four columns of table 3.

The improvement in frequency correlation is shown graphically in figure 9, where the calculated frequencies for the initial and "best fit" support stiffnesses and measured frequencies are plotted against weak direction mode numbers. The torsional spring constant $\overline{K}_T$ was found to be the only effective

parameter influencing higher modes. The rotational spring constant $\bar{K}_R$ influenced only low modal frequencies.

As seen in figure 9(c), the initial calculated frequencies for panel 4 (clips attached to the panel only by the two outer screws) compared reasonably to measured frequencies. This reinforced the assumption that the calculated panel stiffnesses were correct, and that for clips attached by three screws, frequency discrepencies were due to the underestimation of support stiffnesses.

Panels 2 and 3 were identical except that different sides were exposed to the flow. One would expect identical frequency responses. However, the vibration tests have indicated consistently different behavior, especially for second and higher modes and is reflected in the different "best fit" stiffness values of supports. These differences are not fully understood but are attributed to panel warpage and to slight variations in support attachments.

Similar difficulty in natural frequency correlation for corrugated panels was experienced previously by other investigators (ref. 4).

Experimental Flutter Results

Flutter boundaries as a function of yaw angle for all panels listed in table 2 are presented in figures 10 through 15. Because of wind tunnel dynamic pressure limitations, no flutter points were reached between 0° and 15°, and in most cases flutter was obtained only between 30° and 90°. An unusually small amount of data scatter was encountered. This is attributed to: (1) the ease of initiating and stopping flutter by rotating the turntable; and (2) the small temperature effects due to the type of panel design, in which thermal expansion was accommodated by beads and discrete flexible supports.

As can be seen in figures 10 through 15, yaw angle has a considerable effect on the flutter speed of each of the panels tested. For example, in figure 13, the rotation of panel 3 from 90° (flow in the weak direction) to

35° results in a threefold increase in flutter λ. If the yaw angle is decreased further, greater increase in flutter speed may be realized.

In addition to the panels listed in table 2, an attempt was made to obtain flutter boundaries for two isotropic panels having a length-to-width ratio of five. These panels, of 0.0305 cm (0.012 in.) and 0.0406 cm (0.016 in.) thicknesses, were mounted in the same supporting plate as used for the single corrugation panel. No consistent flutter points were obtained, however, due to the constantly changing temperatures which induced buckling of the panels.

Other difficulties encountered during testing were with the cavity pressure control and pressure variations over the panels. At M = 1.6, and at M = 2.0 at low dynamic pressures, leakage around the turntable was too high to permit satisfactory manual control of the cavity pressure. For this reason, the normalized flutter dynamic pressures (q/β) shown in figure 10 are higher at M = 1.6 than at M = 2.0, despite the fact that reference 5 suggests that the M = 1.6 boundary should be below the M = 2.0 curve. Also, due to higher pressure variations over the panels at high dynamic pressures (see figure 6), experimental flutter trends at low yaw angles were more difficult to define. This was especially true for panel 4, which had the lowest support stiffness. (See figure 14).

Considering all of the above factors, the M = 2 results were judged superior to the M = 1.6 results, and accordingly the former were used for correlation with theory.

Correlation with Theory

The flutter analysis used for comparison with the experimental data is a generalization to account for flow angularity of the procedure due to reference 3. This is a Galerkin-type solution for an orthotropic panel on continuous deflectional, rotational, and torsional springs along two opposite

edges, and simply supported along the other two sides. Pressure loading is obtained using static aerodynamics. Flutter is defined as the lowest dynamic pressure corresponding to a coalescence of any two modes. Numerical results presented here represent converged values using as many as thirty modes.

At this point, it should be emphasized that the above analysis requires two opposite sides of the panel to be simply supported, whereas, for the test panels these sides were clamped. For the square panels (panels 2 through 5), this approximation is certainly valid, since the effective length of the panel in the y direction is extremely large, and the x edges do not influence either the panel natural frequencies or panel flutter dynamic pressures. For panel 1, which has four clamped sides, it was found that the best flutter results, at least for the range of yaw angle where test data was available, were obtained by making the short rather than the long sides simply supported. These results are presented in figure 11, where in addition, flutter points at $\Lambda = 0°$ and $90°$ for a clamped-clamped analysis (reference 6) are shown. At $\Lambda = 90°$, λ_{cr} is the same whether the y-edges are simply supported or clamped.

For panel 4, for which initially good frequency correlation was obtained, good flutter comparisons between test and analysis are also evident (figure 14) for the very limited range of yaw angle. The deviation of test values at lower angles can be attributed, as stated previously, to the buildup of pressure loading at these dynamic pressure levels (see figure 6(a)).

For all other panels, correlation is not as good. The discrete flexible supports introduce an additional set of variables having a large influence on flutter. Calculated flutter speeds at high yaw angles are particularly sensitive to the torsional stiffness of the supports. This is illustrated in figure 13, where the calculated flutter parameter λ_{cr} is plotted for $\overline{K}_T = 0.016$ and $\overline{K}_T = 0.30$. $\overline{K}_T = 0.016$ is the value calculated using strain energy methods for one clip and dividing the value by clip spacing. $\overline{K}_T = 0.30$ represents the "best fit" value based on test natural frequencies. The λ_{cr} at $\Lambda = 90°$ is six times greater for $\overline{K}_T = 0.30$ than for $\overline{K}_T = 0.016$. Because of this wide range of possible calculated values, it was felt that a more realistic

approach to correlation would be to present both of the calculated flutter boundaries with the test results. Thus for panels 2, 3 and 5, two analytical flutter boundaries and one experimental boundary are given in figures 12, 13, and 15, respectively.

Test results for panels 3 and 5, in figures 13 and 15, fall between the two analytical flutter points at $\Lambda = 90°$ and approach the upper boundary at lower yaw angles. Thus correlation improves at small and moderate yaw angles where the effect of torsional spring supports is smaller. Repeatability of test results is very evident for these two similar panels. It should be noted that for both panels corrugations are exposed to the flow.

The configuration of panel 2 is identical to panel 3 except that the flat sheet is exposed to the air flow. The test flutter boundaries (figs. 12 and 13) are, however, quite different. λ_{cr} values for panel 2 are less than a third of those for panel 3. Some of the difference can be explained by the different "best fit" stiffness characteristics as shown in table 2. However, it should be noted that panel 2 is the only one for which the test flutter boundary falls below the lower analytical boundary. This implies that panel beading is beneficial for panel flutter.

A possible reason for the "best fit" flutter boundaries falling above the test data for large yaw angles is the overestimation of D_{12} for the double skin panels. Reference 2 indicates that the correlation of the calculated D_{12} with test values is highly dependent on the type of cross-section. Furthermore, cross-sections of the test panels in this investigation are open at the ends and accordingly their full torsional stiffness is not developed until some distance from the supports.

Flutter frequencies were measured concurrently with the flutter dynamic pressures. The comparison of experimental and theoretical flutter frequencies is shown in figure 16 for panels 1, 2, 4, and 5. As expected, good correlation was obtained for panel 1. For the other panels good correlation only exists where the test λ_{cr} is close to the calculated λ_{cr}. This reinforces the

contention that mode coalescence is the flutter mechanism.

It should be noted that the analytical flutter point at $\Lambda = 0°$ is the coalescence of the first two modes in the strong (x) direction, and as such represents perfect alignment of the air flow with the corrugations. Any deviation will involve modes in the weak (y) direction (m = 1, n = 1,2,3), and will lower the flutter speed and flutter frequency. Therefore, it is unrealistic to expect to reach experimentally the analytical λ_{cr} at $\Lambda = 0°$ for orthotropic panels with large $\frac{D_{12}}{D_2}$ ratios.

CONCLUSIONS

Flutter characteristics of two types of corrugation-stiffened panels at various yaw angles were studied both experimentally and analytically. Flutter tests were made at Mach number 2 and 1.6. Analyses were based on quasi-steady aerodynamics. In addition, vibration tests and analyses were performed.

The experimental part of the study has shown that reliable panel flutter results can be obtained if care is taken in eliminating thermal stresses in panel models. A unique feature of this study was the use of a remotely controlled turntable to rotate test panels. Rotating the test panel to initiate and stop flutter clearly delineated the onset of flutter. The results indicate that flutter speed for corrugated panels is highly dependent on yaw angle.

For moderate yaw angles, when a large component of the flow is along the corrugations, correlation with theory was good, but as the flow became perpendicular to the corrugations, large discrepencies between test and theory are apparent. Since for this configuration flutter is extremely sensitive to boundary conditions, a better definition of the structure is needed.

It can also be concluded that beaded surfaces have a stabilizing effect on flutter, though their exact influence is difficult to determine because of the large effect of other parameters.

REFERENCES

1. Bohon, Herman L., and Shore, Charles P.: Application of Recent Panel Flutter Research to the Space Shuttle - Part II, Influence of Edge Clips and Flow Angularity. NASA TM X-2274, Volume III, April 1971.

2. Stroud, W. Jefferson: Elastic Constants for Bending and Twisting of Corrugation-Stiffened Panels. NASA TR R-166, 1963.

3. Heard, Walter L., Jr., and Bohon, Herman L.: Natural Vibration and Flutter of Elastically Supported Corrugation-Stiffened Panels - Experiment and Theory. NASA TN D-5986, October 1970.

4. Carden, Huey D., Durling, Barbara J., and Walton, William C., Jr.: Space Shuttle TPS Panel Vibration Studies. NASA TM X-2274, Volume III, April 1971.

5. Lemley, Clark E.: Design Criteria for the Prediction and Prevention of Panel Flutter. AFFDL-TR-67-140, Volume I, August 1968.

6. Erickson, Larry L.: Supersonic Flutter of Flat Rectangular Orthotropic Panels Elastically Restrained Against Edge Rotation. NASA TN D-3500, August 1966.

Table 1 Panel Types

Corrugation Type	Cross-Section	a cm (in)	$\frac{a}{b}$	D_2 N-cm (lb-in)	$\frac{D_1}{D_2}$	$\frac{D_{12}}{D_2}$
Single Skin	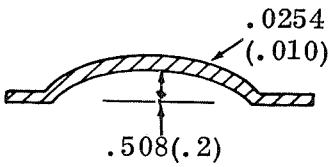	57.2 (22.5)	5.0	9.82 (.88)	755	1.5
Double Skin	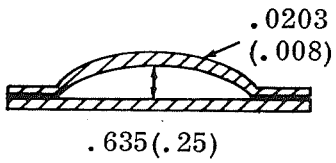	35.6 (14.0)	.935	40.5 (3.58)	420	137
Double Skin	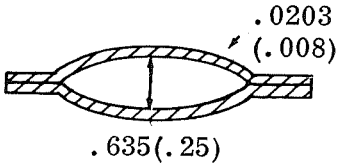	35.6 (14.0)	.935	40.5 (3.58)	270	146

Table 2 Panel Flutter Models

Panel No.	Currugation Type	a cm (in.)	$\frac{a}{b}$	D_2 N-cm (lb-in.)	$\frac{D_1}{D_2}$	$\frac{D_{12}}{D_2}$	Support Along y-Edges*	Calculated Support Stiffnesses	Support Stiffnesses for "Best Fit"
1	Single Skin	57.2 (22.5)	5.0	9.82 (0.88)	755	1.5	clamped	$\overline{K}_D = \infty$ $\overline{K}_R = \infty$	Not Applicable
2	Double skin: Flat sheet joined with corrugation sheet. Flat sheet exposed to airflow.	35.6 (14.0)	.933	40.5 (3.58)	420	137	.0595(.024) clips with 3 screws	$\overline{K}_D = 1.12$ $\overline{K}_R = .022$ $\overline{K}_T = .016$	$\overline{K}_D = 1.12$ $\overline{K}_R = 1.9$ $\overline{K}_T = .12$
3	Double skin: Flat sheet joined with corrugated sheet. Corrugated sheet exposed to airflow	35.6 (14.0)	.933	40.5 (3.58)	420	137	.0595 (.024) clips with 3 screws	$\overline{K}_D = 1.12$ $\overline{K}_R = .022$ $\overline{K}_T = .016$	$\overline{K}_D = 1.12$ $\overline{K}_R = .022$ $\overline{K}_T = .30$
4	Double skin: Flat sheet joined with corrugated sheet. Flat sheet exposed to airflow.	35.6 (14.0)	.933	40.5 (3.58)	420	137	.0595 (.024) clips with 2 screws	$\overline{K}_D = .245$ $\overline{K}_R = .013$ $\overline{K}_T = .008$	$\overline{K}_D = .245$ $\overline{K}_R = .013$ $\overline{K}_T = .008$
5	Double skin: Two joined corrugated sheets.	35.6 (14.0)	.933	40.5 (3.58)	270	146	.0457(.018) clips with 3 screws	$\overline{K}_D = .692$ $\overline{K}_R = .014$ $\overline{K}_T = .007$	$\overline{K}_D = .692$ $\overline{K}_R = .014$ $\overline{K}_T = .30$

*Except for panel 1, x-edges are assumed to be simply supported.

Table 3 Panel Natural Frequencies

Panel No.	n / m	Measured, Hz				Calculated, Hz								Calculated "Best Fit", Hz			
		1	2	3	4	1		2		3		4		1	2	3	4
						S-C	C-C	S-C	C-C	S-C	C-C						
1	1 2 3	152 270 523	347	696		110 225 450	150 328 618	270	296	530	545			Not applicable.			
2	1 2 3	120	136	166	255	104 222		117		134		162		115	137	165	205
3	1 2 3	116 310	160	200	285	104 222		117		134		162		111 261	147	196	254
4	1 2 3	58	73	85	110	56		64		84		120		56	64	84	120
5	1 2 3		124	165	202	71		79		96		127		80	114	158	211

S-C = Simply supported - Clamped
C-C = Clamped - Clamped

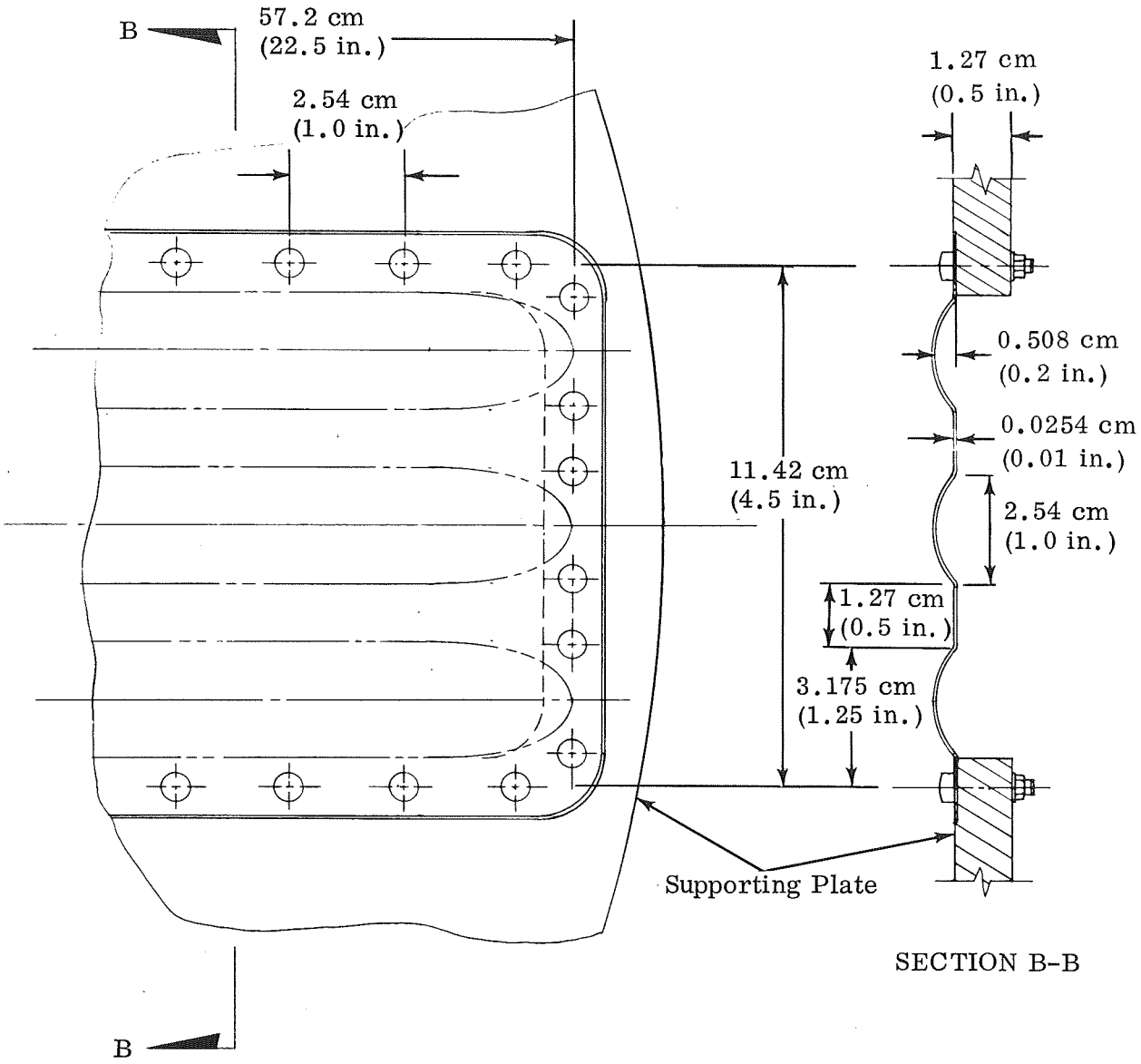

Scale: 1 cm = 1.5 cm

Figure 1 Single Skin Panel

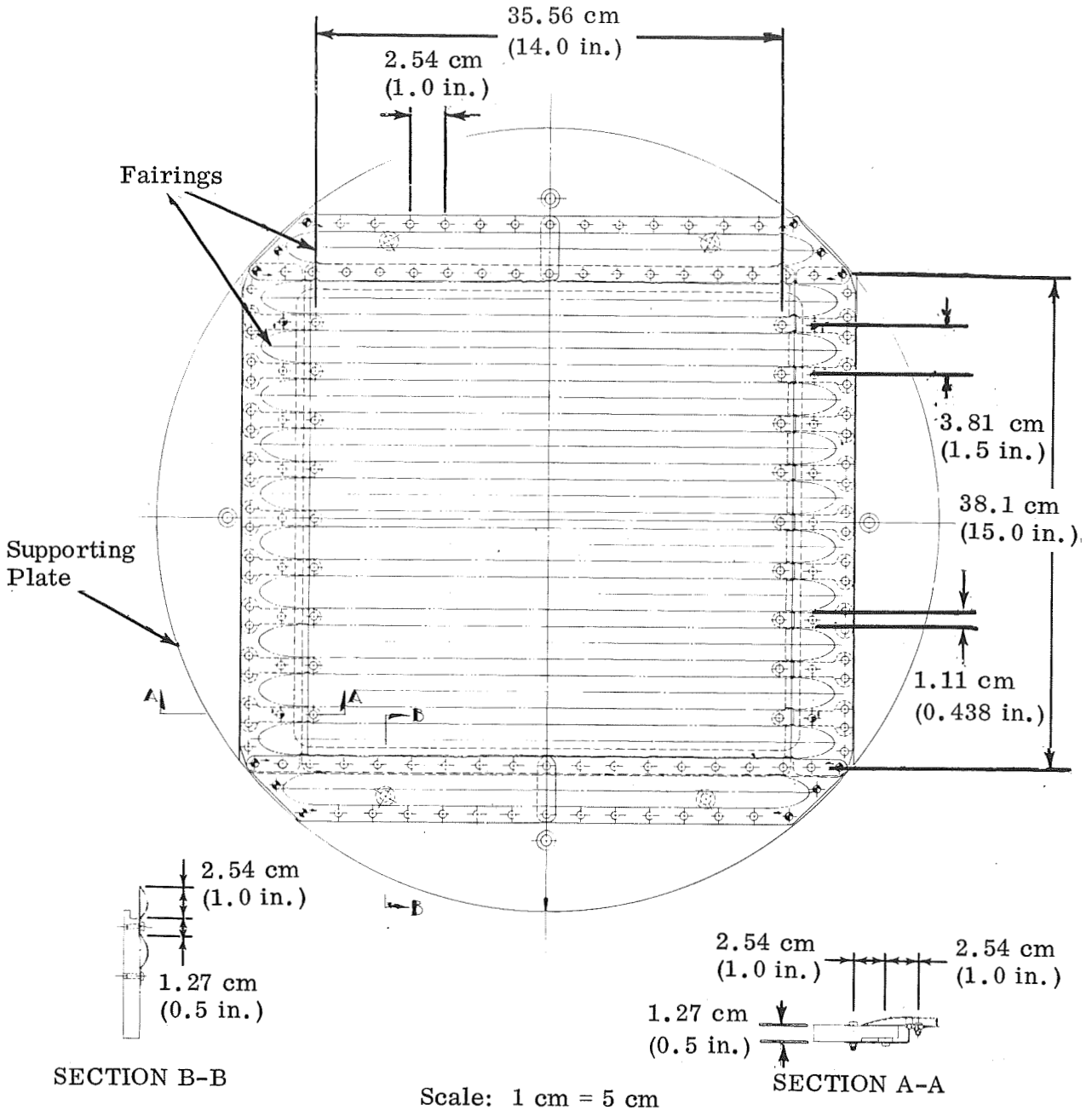

Figure 2 Double Skin Panel

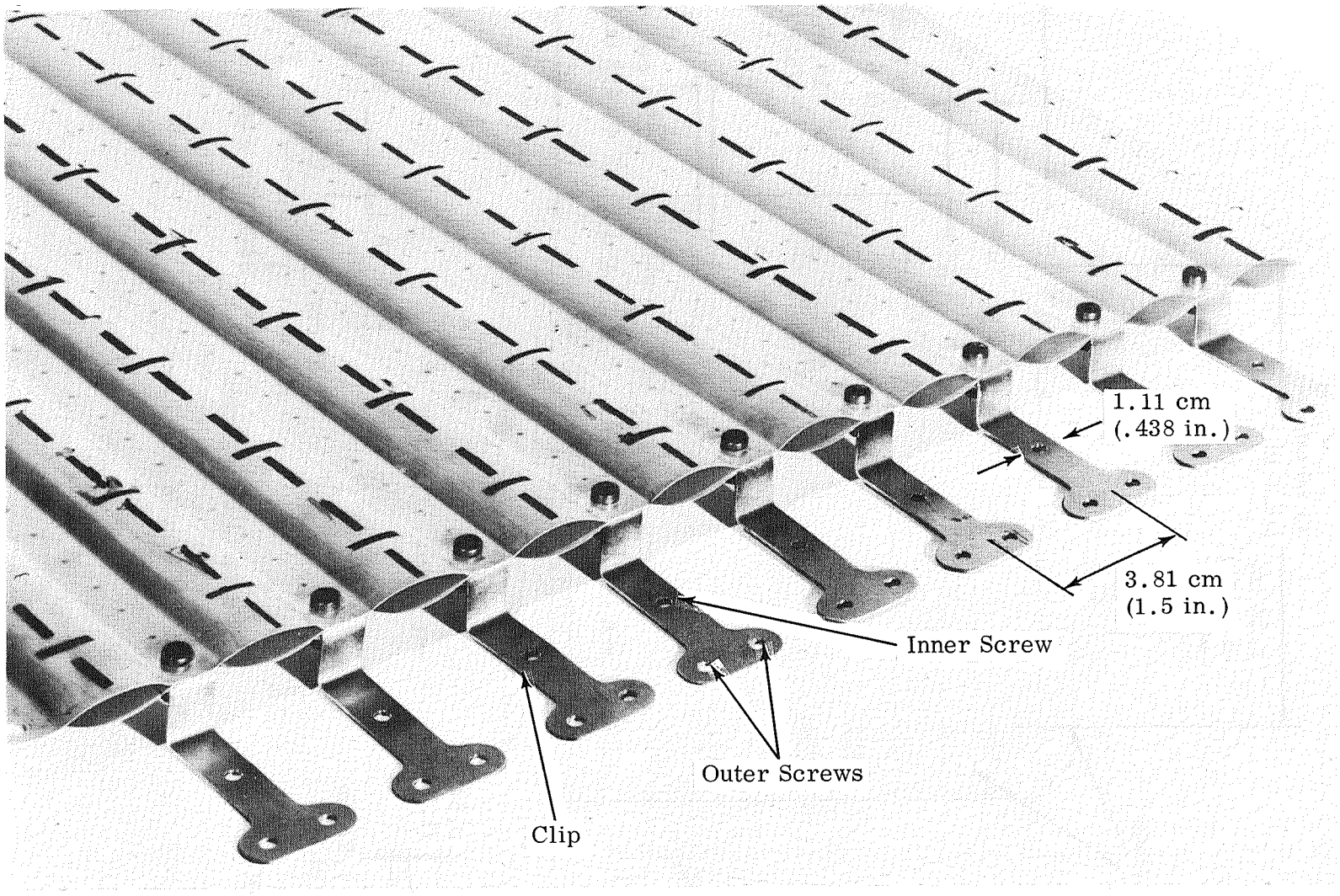

Figure 3 Flexible Support System

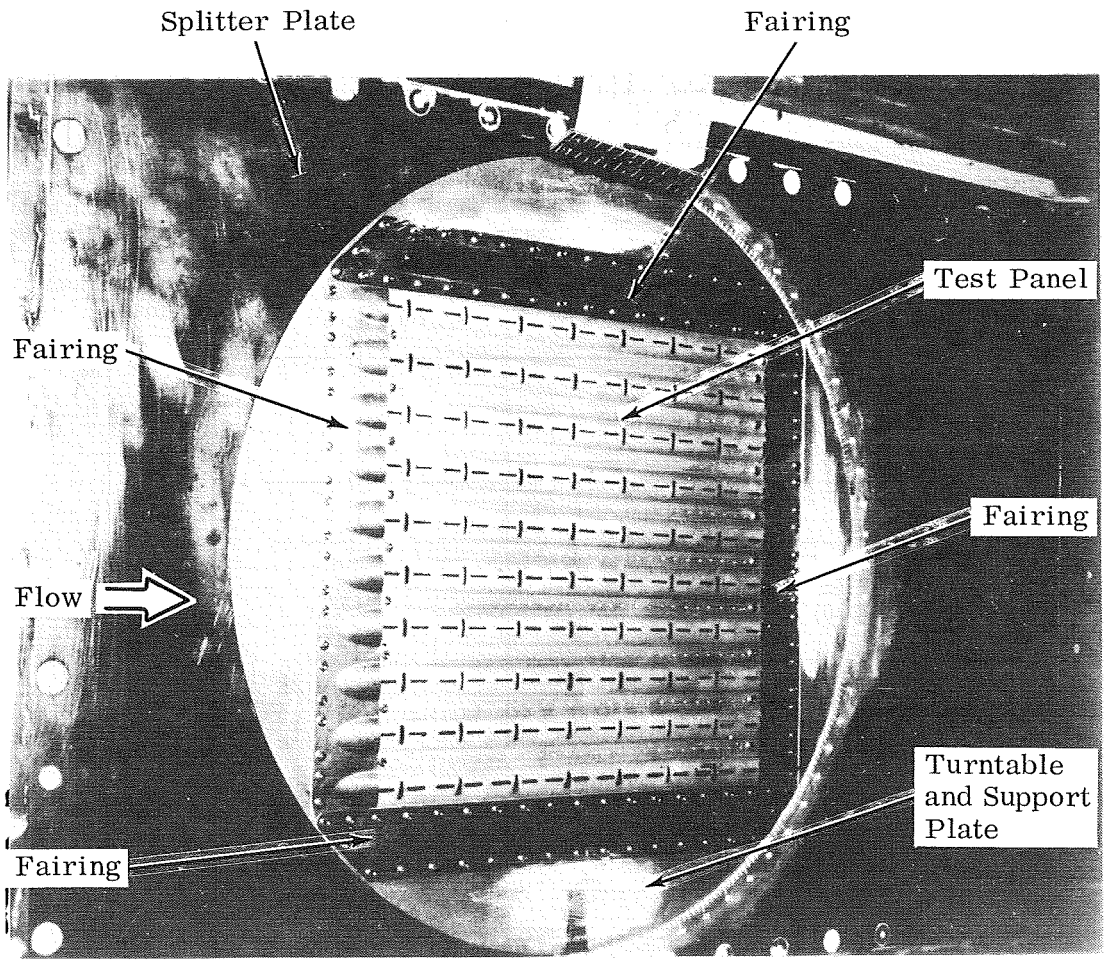

Figure 4 Double Skin Panel Mounted in the Splitter Plate

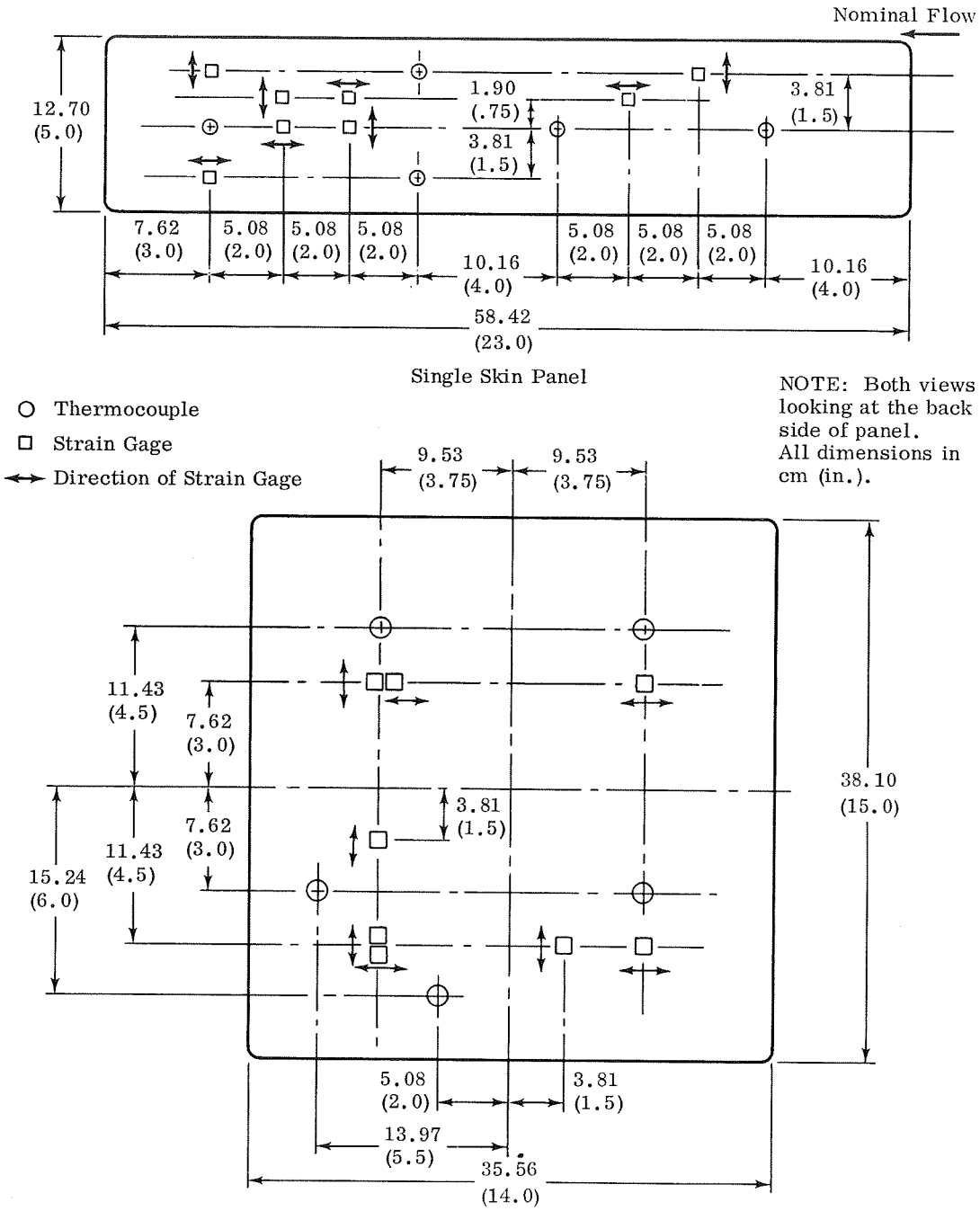

Figure 5 Instrumentation Locations

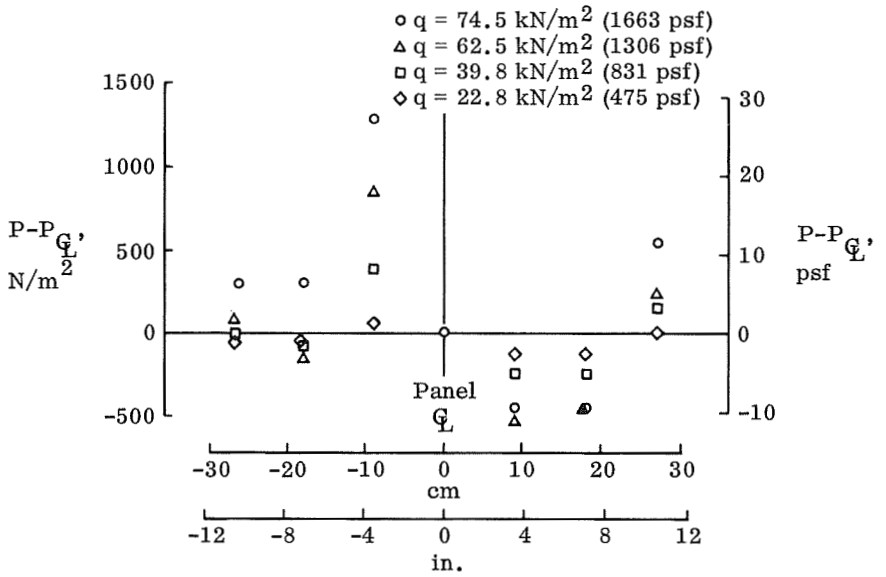

(a) M = 2.0

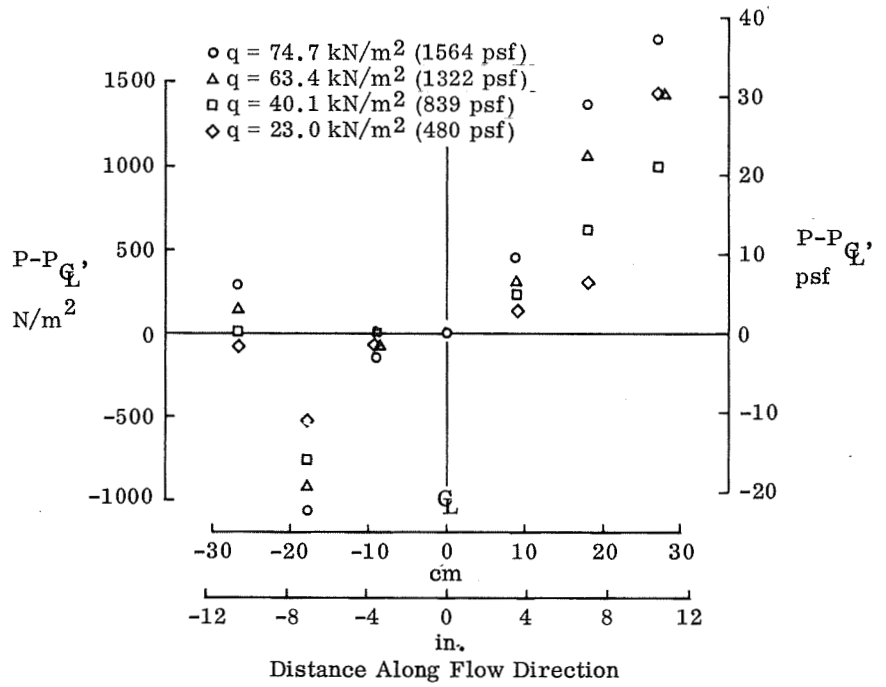

(b) M = 1.6

Figure 6 Pressure Differential Along Centerline of Turntable for Zero Pressure Differential at Center of Turntable at M = 2 and M = 1.6

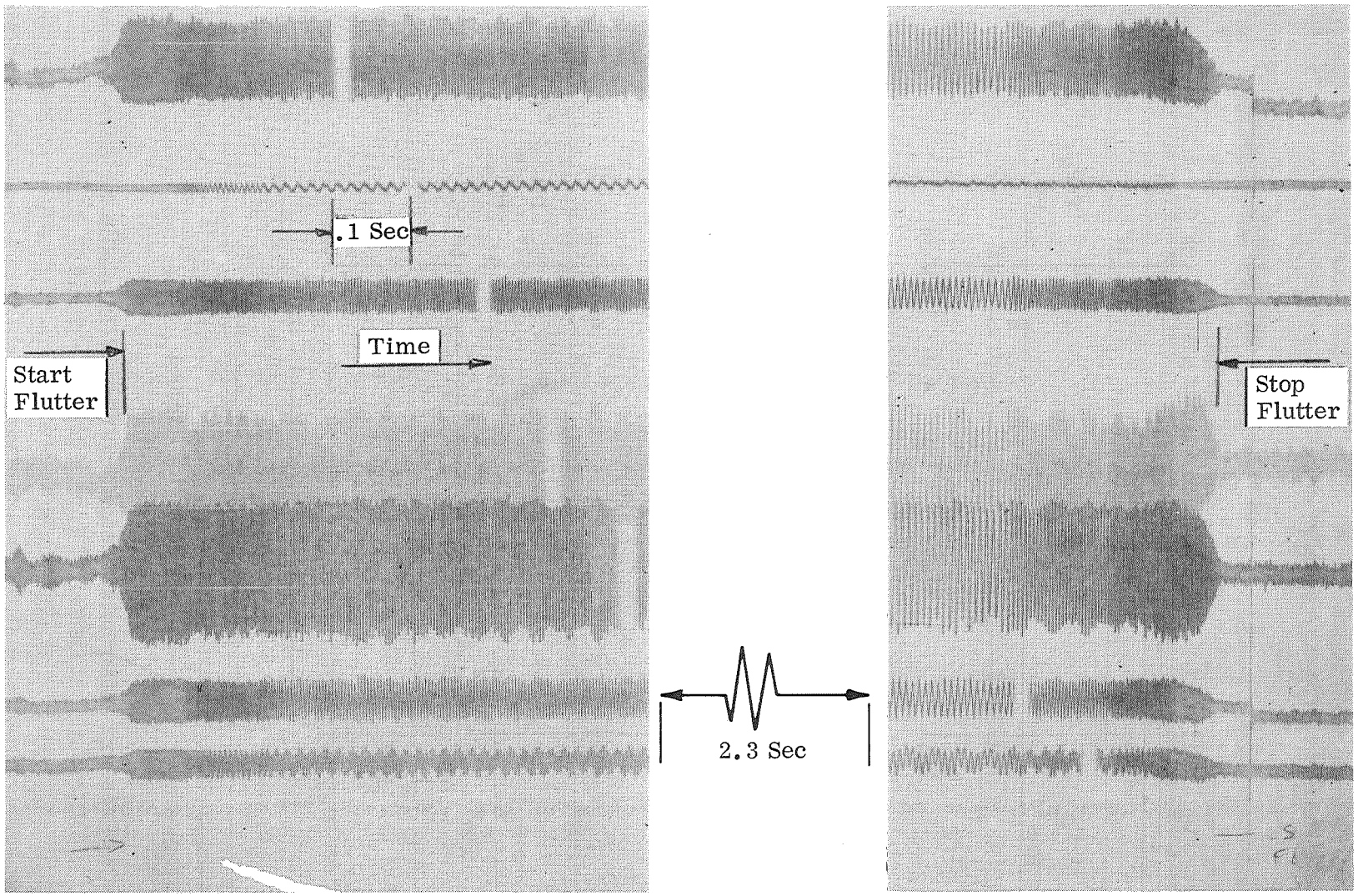

Figure 7 Strain Gage Response During Flutter

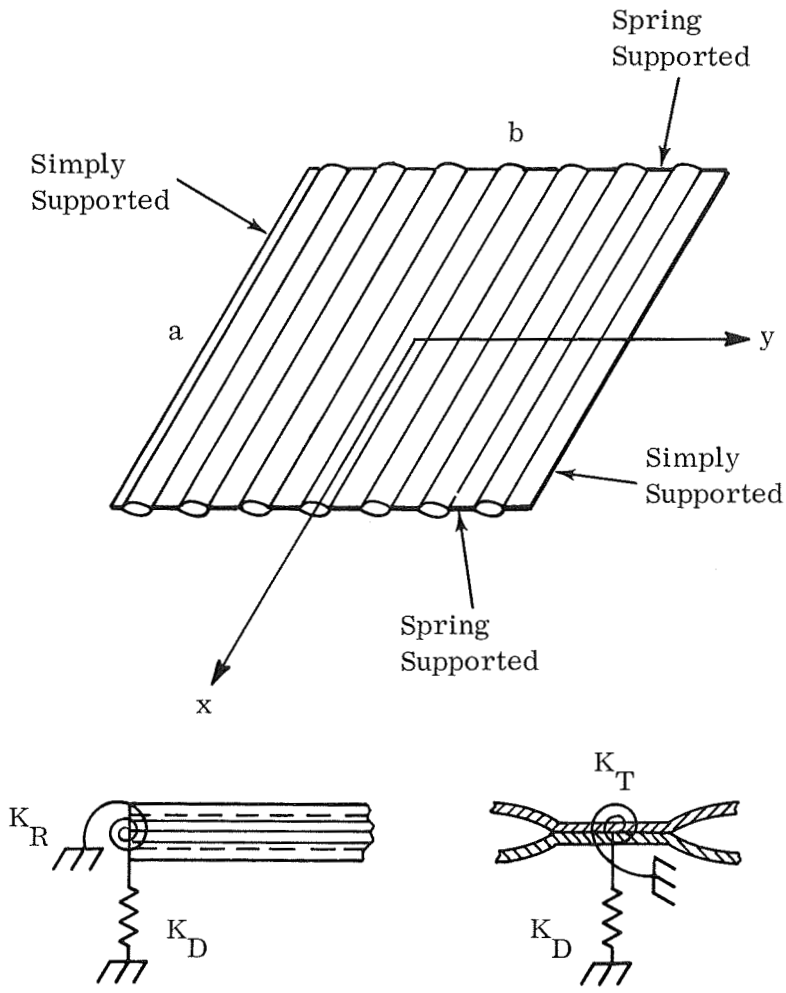

Detail of Spring Support System at $x = \pm \frac{a}{2}$ edges

Figure 8 Schematic of Orthotropic Panel and Support System

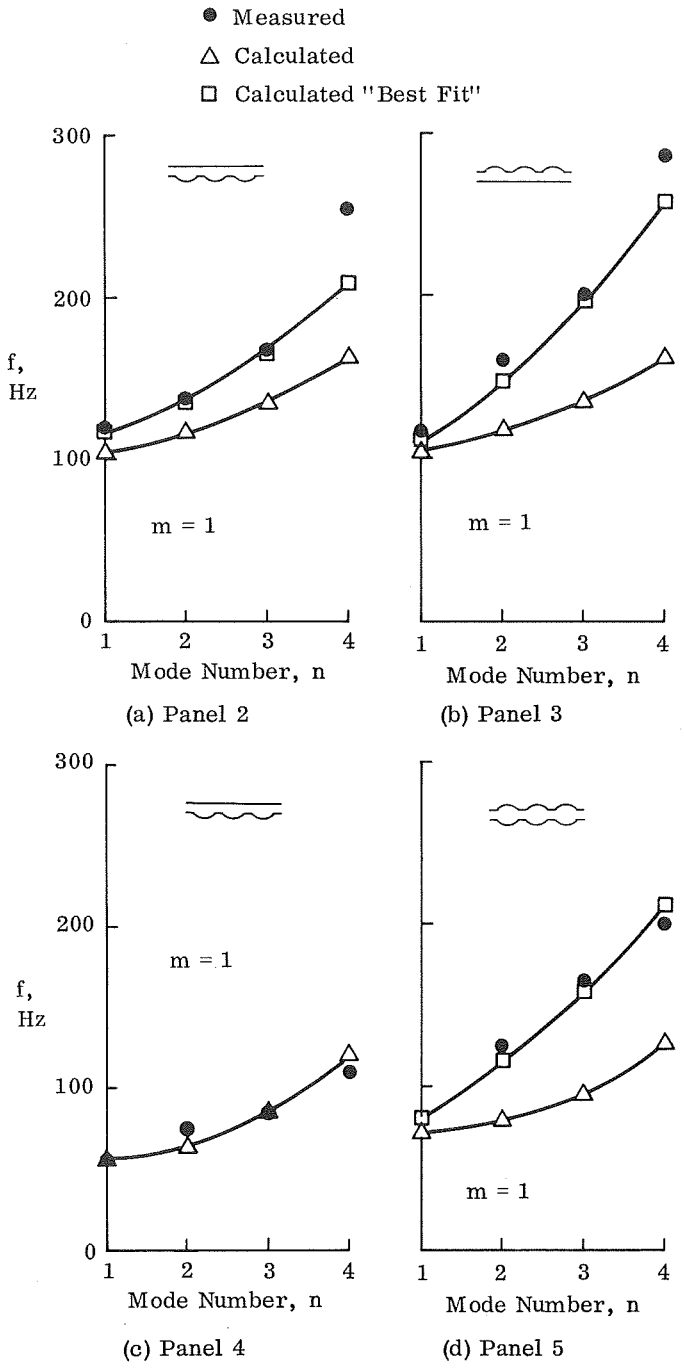

Figure 9 Comparison of Experimental and Theoretical Weak-Direction Panel Natural Frequencies

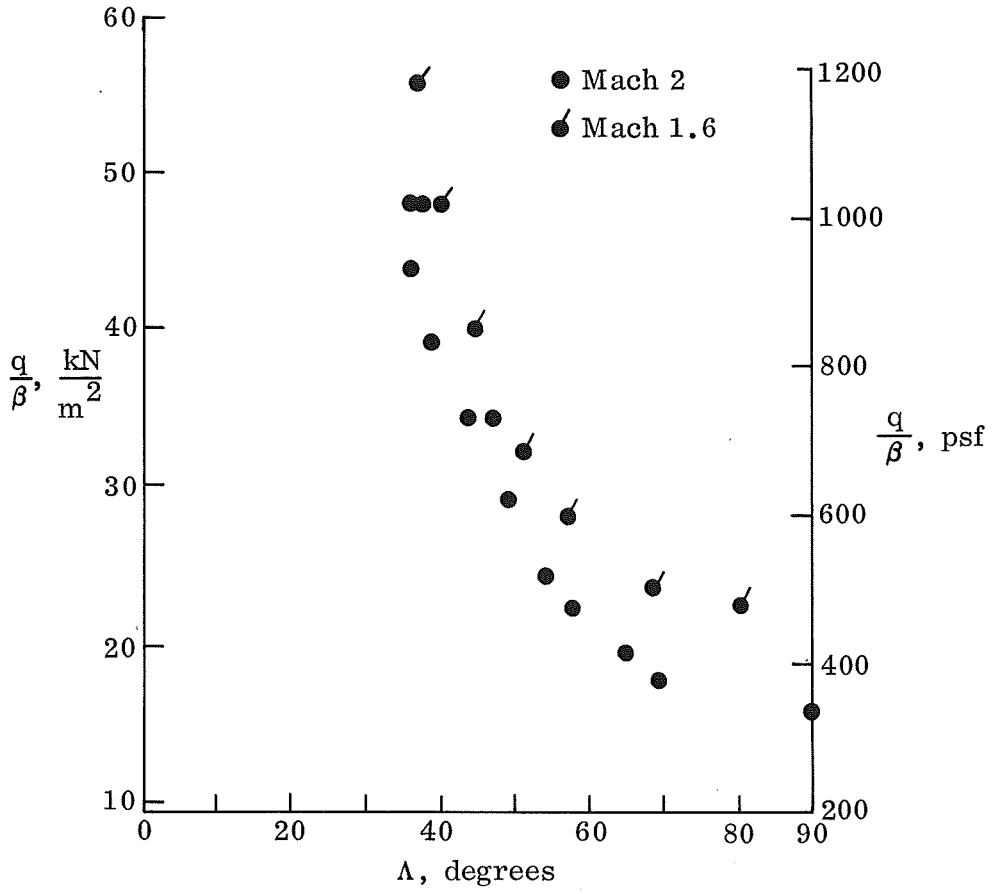

Figure 10 Comparison of Experimental Flutter Boundaries at M = 2 and M = 1.6 for Panel 3

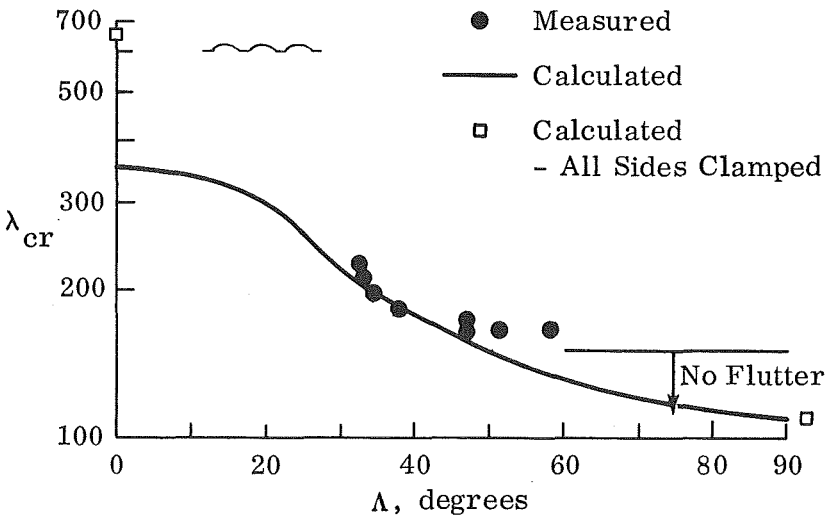

Figure 11 Comparison of Experimental and Theoretical Flutter Boundaries for Panel 1 at M = 2.0

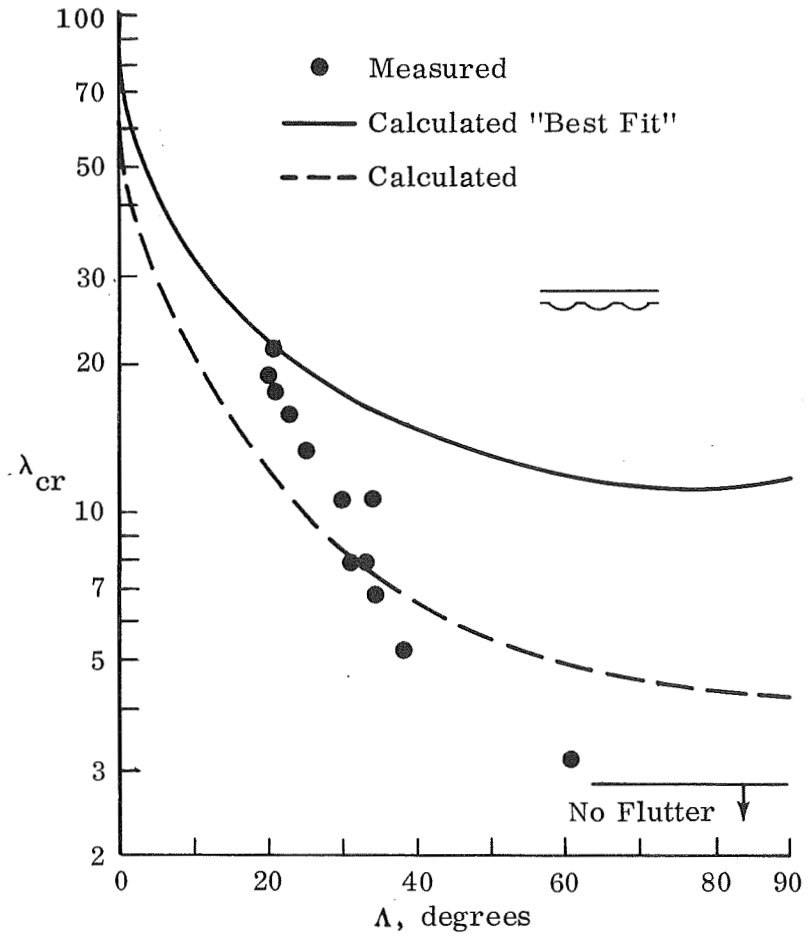

Figure 12 Comparison of Experimental and Theoretical Flutter Boundaries for Panel 2 at M = 2.0

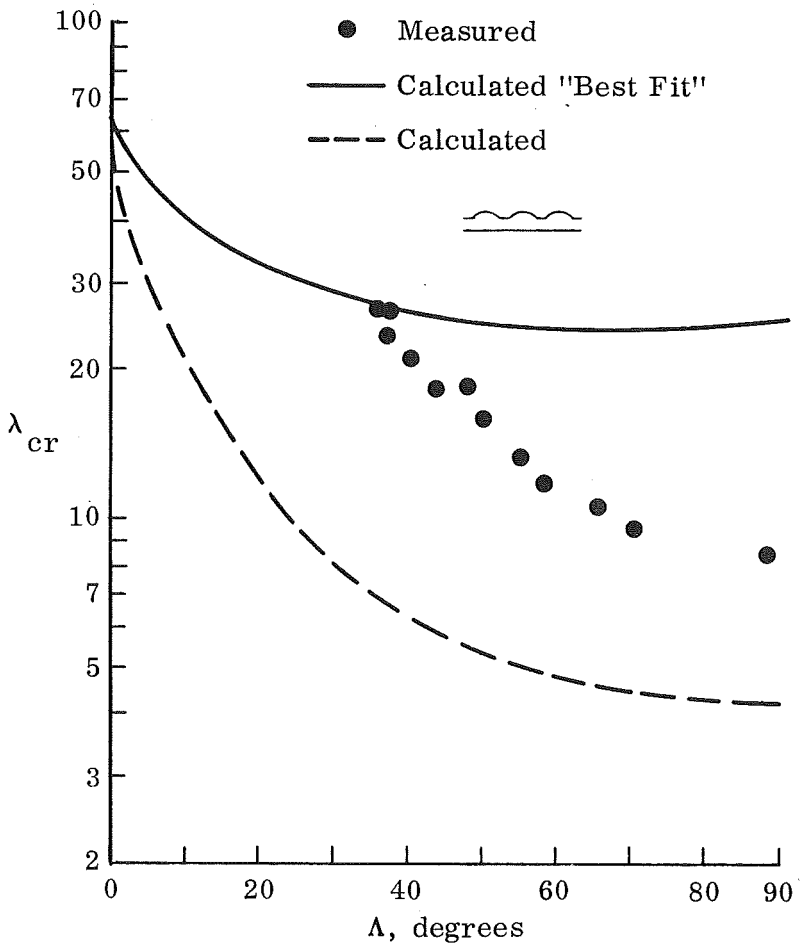

Figure 13 Comparison of Experimental and Theoretical Flutter Boundaries for Panel 3 at M = 2.0

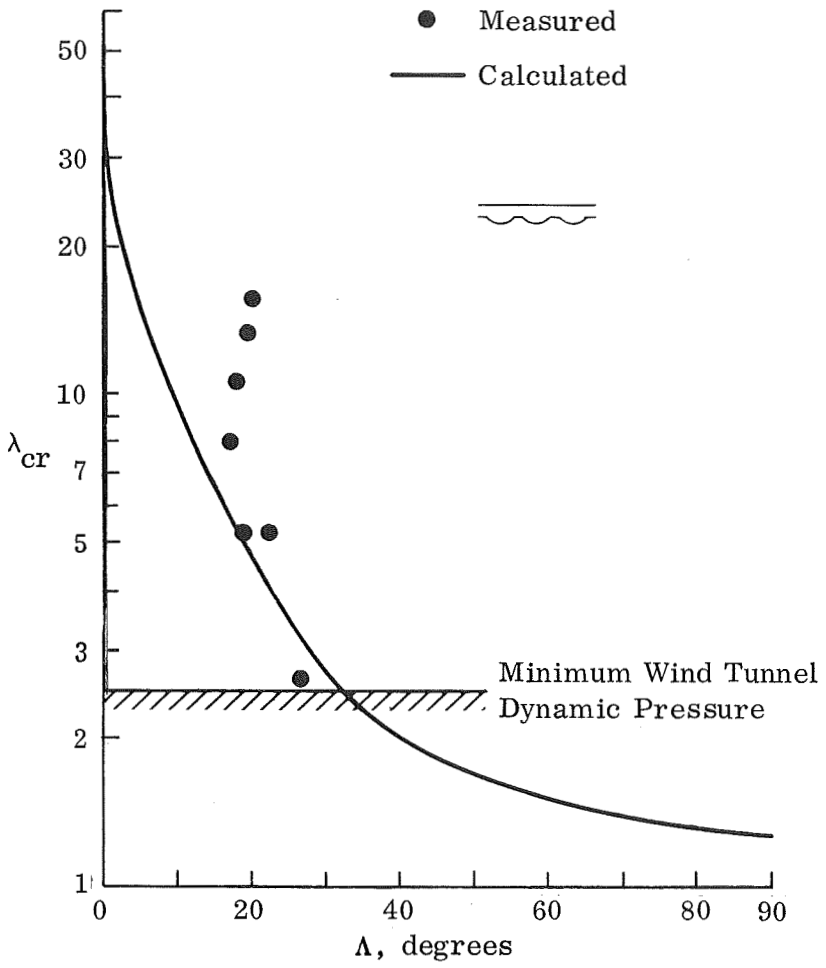

Figure 14 Comparison of Experimental and Theoretical Flutter Boundaries for Panel 4 at M = 2.0

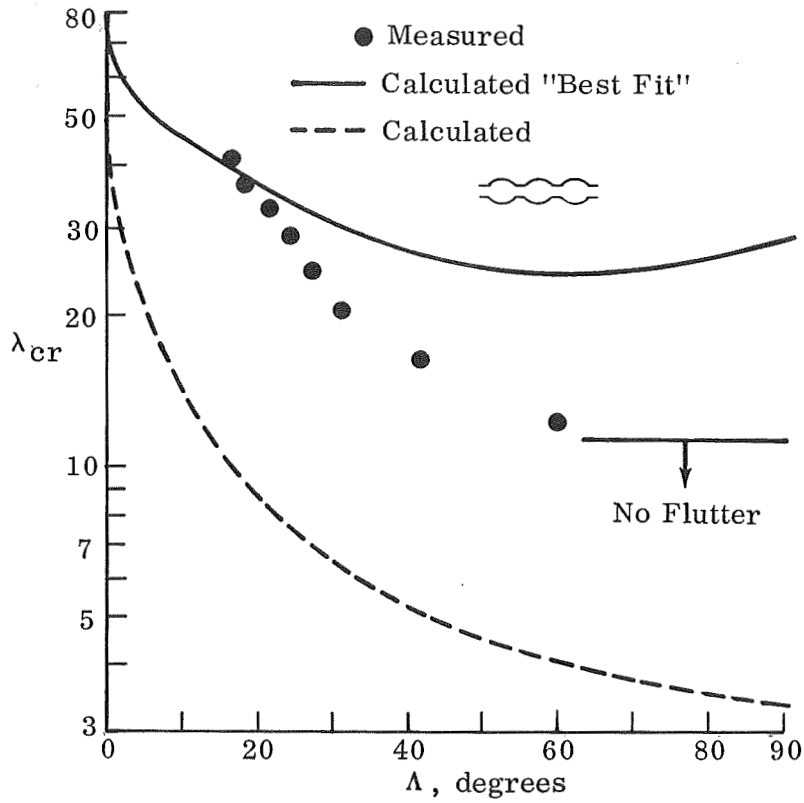

Figure 15 Comparison of Experimental and Theoretical Flutter Boundaries for Panel 5 at M = 2.0

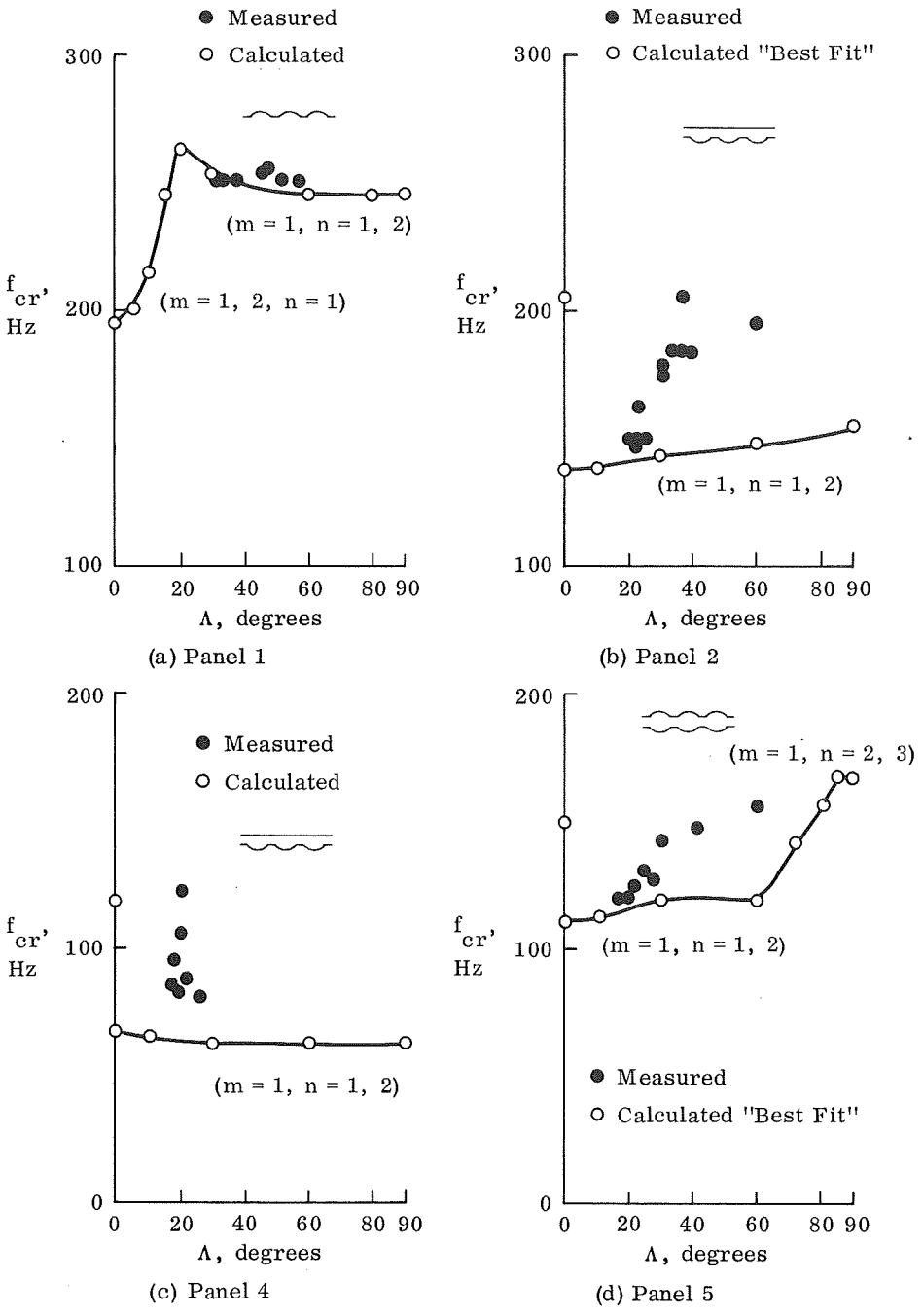

Note: Numbers in parenthesis indicate modes which coalesce

Figure 16 Comparison of Experimental and Theoretical Flutter Frequencies at M = 2

1. Report No.	2. Government Accession No.	3. Recipient's Catalog No.
NASA CR-2265		

4. Title and Subtitle	5. Report Date
EXPERIMENTAL INVESTIGATION OF ORTHOTROPIC PANEL FLUTTER AT ARBITRARY YAW ANGLES, AND COMPARISON WITH THEORY	May 1973
	6. Performing Organization Code
7. Author(s) Peter Shyprykevich	8. Performing Organization Report No.
	10. Work Unit No.
9. Performing Organization Name and Address Grumman Aerospace Corporation Bethpage, New York	11. Contract or Grant No. NAS1-10635-6
	13. Type of Report and Period Covered Contractor Report
12. Sponsoring Agency Name and Address National Aeronautics and Space Administration Washington, D.C. 20546	14. Sponsoring Agency Code

15. Supplementary Notes

16. Abstract

Flutter characteristics for yaw angles between 15° and 90° were determined experimentally for two types of corrugation-stiffened panels: those with weak twisting stiffness and those with strong twisting stiffness. By mounting the panels on a remotely controlled turntable, good definition of the flutter boundaries was obtained by rotating the panels into and out of flutter. Flutter tests were conducted at M = 2 and M = 1.6 in the Langley Unitary Plan Wind Tunnel. Before flutter testing, vibration tests and analyses were also performed. The experimental flutter data is compared with flutter theory for orthotropic panels utilizing quasi-steady aerodynamics. In total, five different corrugated panels were tested consisting of one single skin panel having a length-to-width ratio of 5 on clamped supports and four different square double skin panels on discrete flexible supports. The investigation indicated that flutter speed for corrugated panels is highly dependent on yaw angle. Reasonable flutter correlation between analysis and test was obtained for moderate yaw angles but extreme sensitivity to structural parameters made the correlation at large yaw angles uncertain.

17. Key Words (Suggested by Author(s))	18. Distribution Statement
Panel flutter tests Corrugated panel Corrugation-stiffened panel Panel flutter data at yaw angles Flutter data for yawed panels	Unclassified - Unlimited

19. Security Classif. (of this report)	20. Security Classif. (of this page)	21. No. of Pages	22. Price*
Unclassified	Unclassified	33	$3.00

*For sale by the National Technical Information Service, Springfield, Virginia 22151

NATIONAL AERONAUTICS AND SPACE ADMINISTRATION
WASHINGTON, D.C. 20546

OFFICIAL BUSINESS
PENALTY FOR PRIVATE USE $300

SPECIAL FOURTH-CLASS RATE
BOOK

POSTAGE AND FEES PAID
NATIONAL AERONAUTICS AND
SPACE ADMINISTRATION
451

U.S.MAIL

POSTMASTER : If Undeliverable (Section 158 Postal Manual) Do Not Return

"The aeronautical and space activities of the United States shall be conducted so as to contribute . . . to the expansion of human knowledge of phenomena in the atmosphere and space. The Administration shall provide for the widest practicable and appropriate dissemination of information concerning its activities and the results thereof."

—NATIONAL AERONAUTICS AND SPACE ACT OF 1958

NASA SCIENTIFIC AND TECHNICAL PUBLICATIONS

TECHNICAL REPORTS: Scientific and technical information considered important, complete, and a lasting contribution to existing knowledge.

TECHNICAL NOTES: Information less broad in scope but nevertheless of importance as a contribution to existing knowledge.

TECHNICAL MEMORANDUMS: Information receiving limited distribution because of preliminary data, security classification, or other reasons. Also includes conference proceedings with either limited or unlimited distribution.

CONTRACTOR REPORTS: Scientific and technical information generated under a NASA contract or grant and considered an important contribution to existing knowledge.

TECHNICAL TRANSLATIONS: Information published in a foreign language considered to merit NASA distribution in English.

SPECIAL PUBLICATIONS: Information derived from or of value to NASA activities. Publications include final reports of major projects, monographs, data compilations, handbooks, sourcebooks, and special bibliographies.

TECHNOLOGY UTILIZATION PUBLICATIONS: Information on technology used by NASA that may be of particular interest in commercial and other non-aerospace applications. Publications include Tech Briefs, Technology Utilization Reports and Technology Surveys.

Details on the availability of these publications may be obtained from:

SCIENTIFIC AND TECHNICAL INFORMATION OFFICE

NATIONAL AERONAUTICS AND SPACE ADMINISTRATION

Washington, D.C. 20546